Journal Name

ARTICLE TYPE

Cite this: DOI: 10.1039/xxxxxxxxxx

New approach to understand the NMR relaxivity properties of cobalt ferrite nanoparticles - Electronic Supplementary information†

Anne-Laure Rollet,*[a] Sophie Neveu,[a‡] Patrice Porion,[b‡] Vincent Dupuis,[a‡] Nadine Cherrak,[a‡] and Pierre Levitz[a,c]

Received Date
Accepted Date

DOI: 10.1039/xxxxxxxxxx

www.rsc.org/journalname

The synthesis of ferrite coablt nanoparticles for each set of samples is detailed. The influence of several parameters (the anisotropy constant, the damping factor, the dead layer and the τ_0) used in the model are detailed here. The linear dependences of the relaxation rate versus the volume fraction of MNPs are shown for several temperatures. The Arrhenius plot of the relaxivities at 20MHz is presented and from the linear regression an activation energy is obtained.

1 Ferrite Cobalt nanoparticles samples

The protocol used for each sample is detailed in a table 1. The TEM images and the size distribution for all the samples used in this study are also provided figure 1. The distribution is fitted using a log-normal law:

$$f(d,d_0,\sigma) = \frac{1}{d\sigma\sqrt{2\pi}} exp(-\frac{(lnD - lnD_0)^2}{2\sigma^2}) \quad (1)$$

with σ the standard deviation of the distribution.

Sample	Synthesis	D_{TEM} (nm)	σ_{TEM}
S1	coprecipitation and size-sorting	4.7	0.47
S2	coprecipitation and size-sorting	5.8	0.53
S3	coprecipitation with complexing species	5.9	0.41
S4	coprecipitation with complexing species	6.8	0.43
S5	coprecipitation and size-sorting	7.9	0.44
S6	coprecipitation process	8.5	0.4
S7	coprecipitation process	10.1	0.62
S8	coprecipitation process	10.6	0.44
S9	coprecipitation process	10.6	0.42
S10	coprecipitation and size-sorting	10.7	0.45
S11	hydrothermal process	12.7	0.28
S12	hydrothermal process	16.2	0.28
S13	hydrothermal process	18.7	0.41

Table 1 Samples used in this study.

1.1 Coprecipitation process

$CoFe_2O_4$ nanoparticles are obtained by precipitating Co(II) and Fe(III) hydroxydes followed by a heating at boiling temperature. For a typical synthesis, sodium hydroxide (160 mL, 10 mol.L^{-1}) was abruptly added under vigorous stirring to a solution of cobalt and ferric nitrate (350 mL, [M] = [Fe] + [Co] = 0.44 mol.L^{-1}, [Co] / [Fe] = 0.4). After stirring 30 minutes, a nonmagnetic amorphous suspension was obtained and heated at 100°C for 2 hours. The mixture became magnetic was washed three times with distilled water. The second step to obtain a cobalt ferrite ionic magnetic fluid is the dispersion of the magnetic nanoparticles. In order to stabilize the nanoparticles in neutral aqueous solution, the particles were coated by citrate species. After stirring 30 minutes in citrate solution, citrated magnetic nanoparticles were dispersed in water and the final product was a stable ionic magnetic fluid with a pH around 7. The size of the nanoparticles thus obtained was around 10 nm. We obtained by this process an aqueous magnetic fluid at pH = 7 (samples S6, S7, S8 and S9).

1.2 Coprecipitation and size-sorting

In order to obtain monodisperse magnetic fluid, we used the size sorting process described in ref[1]. This size sorting process is based on the thermodynamical properties of aqueous dispersion of cobalt ferrite synthesized by the coprecipitation process described above. This process allows to fractionate the particle size distribution and to obtain samples S1, S2, S5 and S10.

1.3 Coprecipitation in the presence of complexing species

In order to obtain smaller particles, the coprecipitation process was realized in the presence of complexing species such as tartrate ions as described in reference[2]. The size of the nanoparticles

[a] PHENIX, Sorbonne Universités, UPMC Univ Paris 06, CNRS, Laboratoire de Physico-Chimie des Electrolytes et Nanosystème Interfaciaux (PHENIX) Paris, France.
[b] laboratoire Interfaces, Confinement, MatÃĨriaux et Nanostructures - ICMN Interfaces, Confinement, Matériaux et Nanostructures - ICMN, CNRS, Université Orléans, Orléans, France.
[c] Physique de la Matière condensée (PMC), CNRS, Ecole Polytechnique, Palaiseau, France.

thus obtained was around 5 nm (samples S3 and S4).

1.4 Hydrothermal process

In order to obtain bigger particles, instead of heating at boiling two hours, the hydroxydes were heated in an autoclave at 200 °C, during 24 hours as described in reference[3]. The size of the nanoparticles thus obtained was around 20 nm (samples S11, S12 and S13).

2 Theoritical Model

Here we present the effect of some parameters used in the model. As underlined in the main text, no fit was performed on the experimental data. We have used the values found in the litterature. However, we must stress that some parameters being difficult to measure, they may be a matter of debate. Hence, we show here the influence of these parameters on the different contributions of R_1 (transverse, Curie, and Curie fluctuation), idem for R_2 as well as the total r_1 and r_2. These parameters are: the anisotropy constant, the damping factor, the dead layer, and tau0. We have performed these calculations for a dispersion of 8 nm MNPs in water.

2.1 effect of anisotropy constant

The anisotropy constant appears in $\tau_{//}$ and $\tau_{\perp}$. Hence, both the first and the thrid terms, named transversal and Curie fluctuation terms respectively, of R_1 equation will be influenced. The second term, the Curie term is not affected. When the anisotropy increases, we see in Figure 2, that r_1 and r_2 at low frequency is increased and the bump around 10 MHz disappears. In the expression of R_2, it appears in the first and third terms of the C component and the $V(\omega_I)$ component. The first terms are also named transversal term and the third terms are named the Curie fluctuation terms.

2.2 effect of the damping factor

The damping factor appears in the time $\tau_{\perp}$. Hence, it must have influence only on the first term, named transversal term, of the R_1 equation. In the expression of R_2, it appears in the first term of the C component and in the first term of the $V(\omega_I)$ component. In the text, we have also referred these two terms as transversal term. With no surprised, we see that only the transversal term is influenced by the damping factor. It tends to decreases $R_{1-trans}$ and $R_{2-trans}$ especially at high frequency.

3 NMR relaxation measurement

3.1 R_1 and R_2 dependence in concentration

The relaxivities $r_1 = (R_1/[\mathrm{Fe+Co}])^{-1}$ and $r_2 = (R_2/[\mathrm{Fe+Co}])^{-1}$ were determined using five MNPs dispersions with the iron and

2.3 effect of the dead layer

The dead layer is the non magnetic layer at the surface of the MNPs. In consequence, it affects the magnetic volume of the MNPs that influences all the components of R_1 and R_2.

2.4 effect of the τ_0

The τ_0 parameter is the prefactor of the Neel time expression. It will therefore affect all the component containing the Néel time.
cobalt concentration [Fe+Co] ranging from 0.5 to 20 mM, approximately. In this range, $R_1 = 1/T_1$ and $R_2 = 1/T_2$ varies linearly with [Fe+Co], and the R_1 and R_2 values are obtained with a linear regression. Figure S 6 presents the variation of R_1 and R_2 as a function of the volume fraction ϕ in %. The slope gives a relaxivity in s^{-1} % $^{-1}$ and the conversion factor α , to s^{-1} mM $^{-1}$ is $\alpha = (d\,n)/(100000\,M) = 1.476\ 10^{-3}$ with d the density of cobalt ferrite (5300 kg/m^3), n the number of metal mole (cobalt + iron) in the cobalt ferrite compound and M the molar mass (234.619 g/mol).

3.2 R_1 and R_2 dependence in temperature

The evolution of R_1 and R_2 versus the MNPs volume fraction ϕ is presented for five temperatures (10, 17, 25, 33 and 40 °C). The linear evolution versus ϕ is observed for all the temperatures. This is a good indicator that the dispersion is stable and no aggregation of MNPs occurs. The temperature dependence of R_1 and R_2 for a medium size sample is presented in figures S 7 and S 8, respectively. The Neperian logarithms of R_1 and R_2 vary linearly with $1/RT$. A linear regression is performed in order to get the corresponding activation energy. The variations shown here for a 10.6 nm typify those observed for all samples.

References

1 S. Lefebure, E. Dubois, V. Cabuil, S. Neveu and R. Massart, *J. Mater. Res.*, 1998, **13**, 2975–2981.

2 S. Neveu, A. Bée, M. Robineau and D. Talbot, *J. Colloid Interface Sci.*, 2002, **255**, 293–298.

3 V. Cabuil, V. Dupuis, D. Talbot and S. Neveu, *J. Magn. Magn. Mat.*, 2011, **323**, 1238–1241.

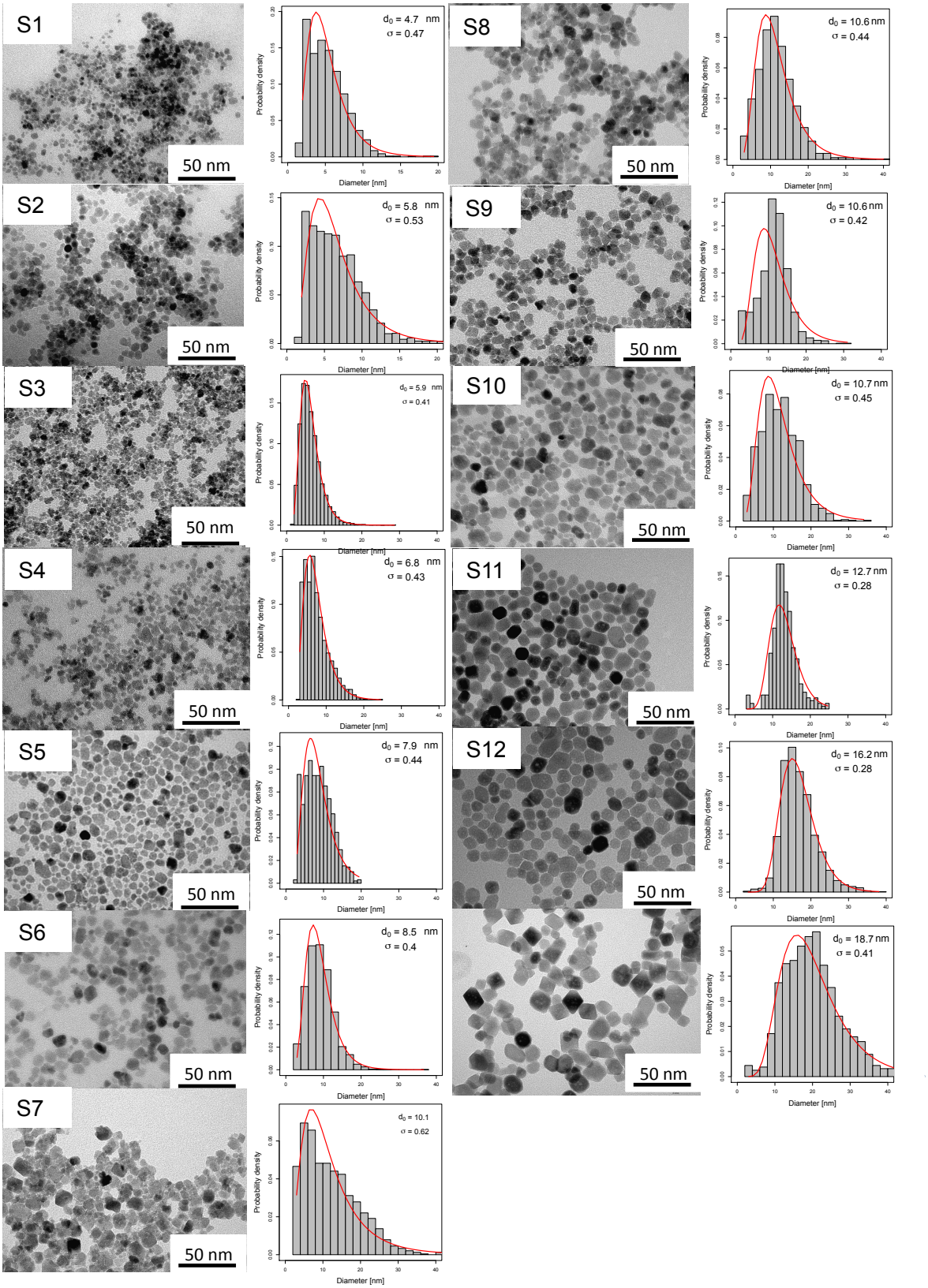

Fig. 1 TEM images and the size distribution for all the samples used in this study (for the name, see table 1).

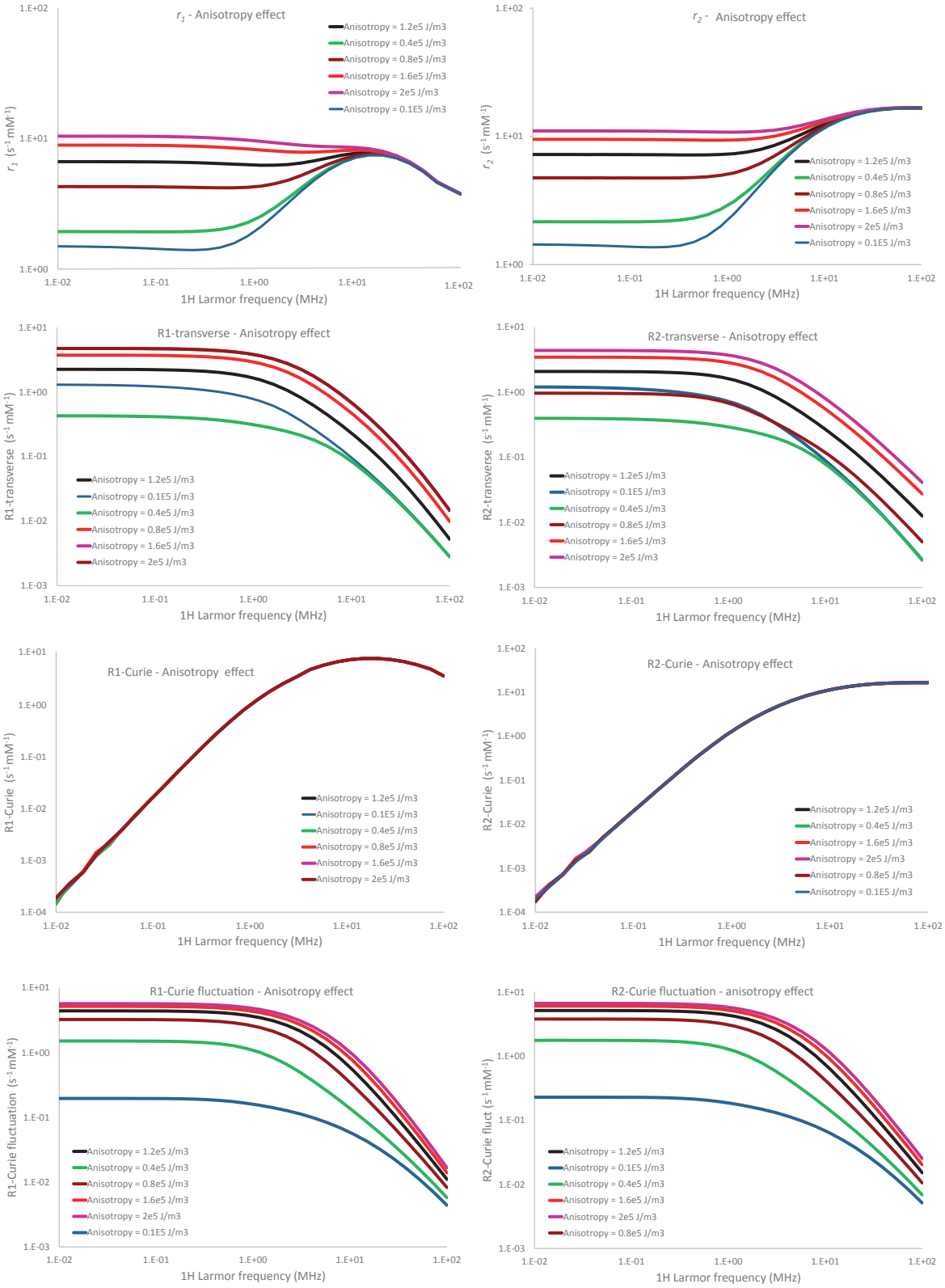

Fig. 2 Effect of the anisotropy constant on the relaxivity r_1 on the left (top) and on the relaxivity r_2 on the right (top), as well as its effect on the three components (transversal term, Curie term and Curie fluctuation term).

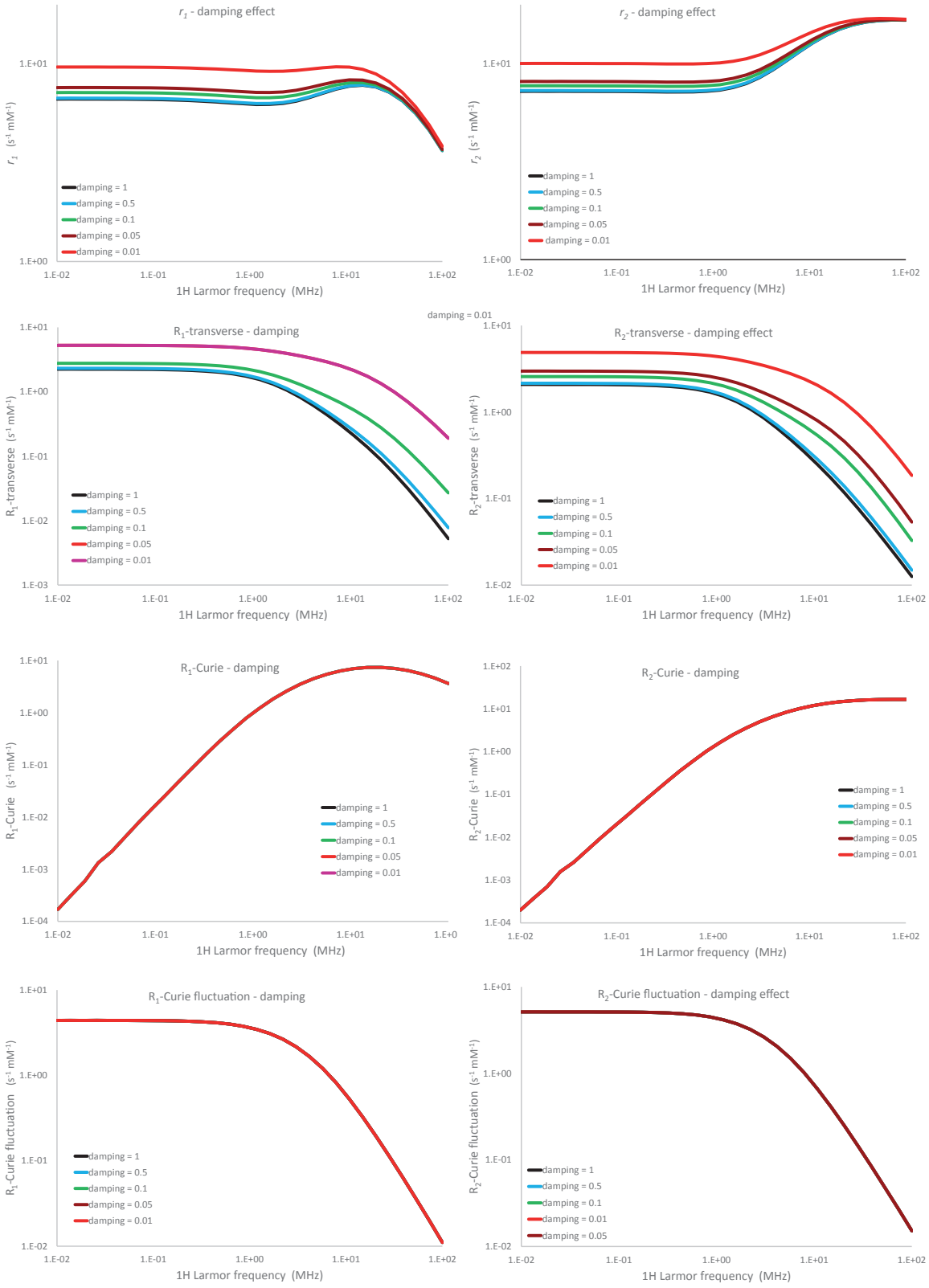

Fig. 3 Effect of the damping factor on the relaxivity r_1 on the left (top) and on the relaxivity r_2 on the right (top), as well as its effect on the three components (transversal term, Curie term and Curie fluctuation term).

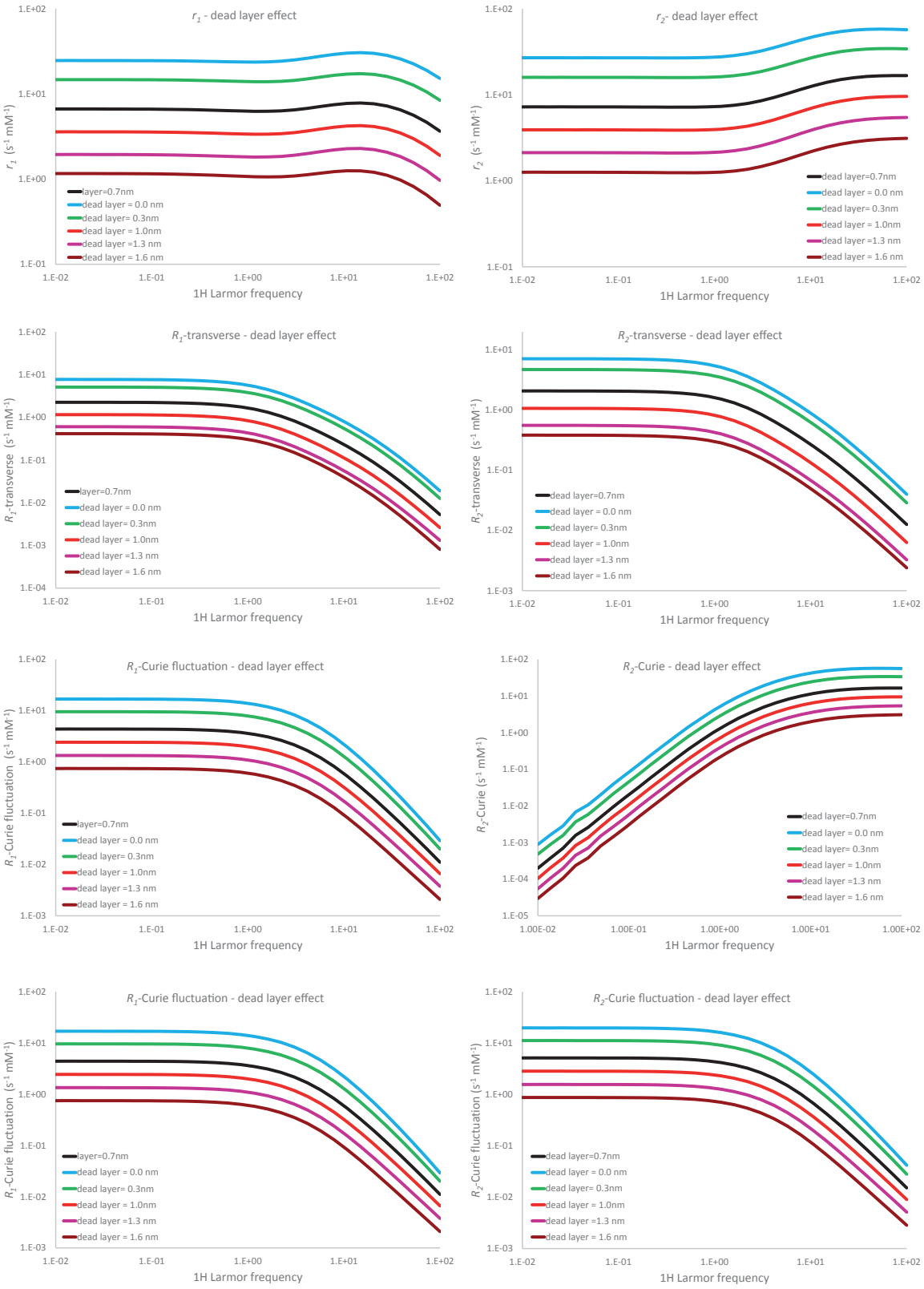

Fig. 4 Effect of the dead layer on the relaxivity r_1 on the left (top) and on the relaxivity r_2 on the right (top), as well as its effect on the three components (transversal term, Curie term and Curie fluctuation term).

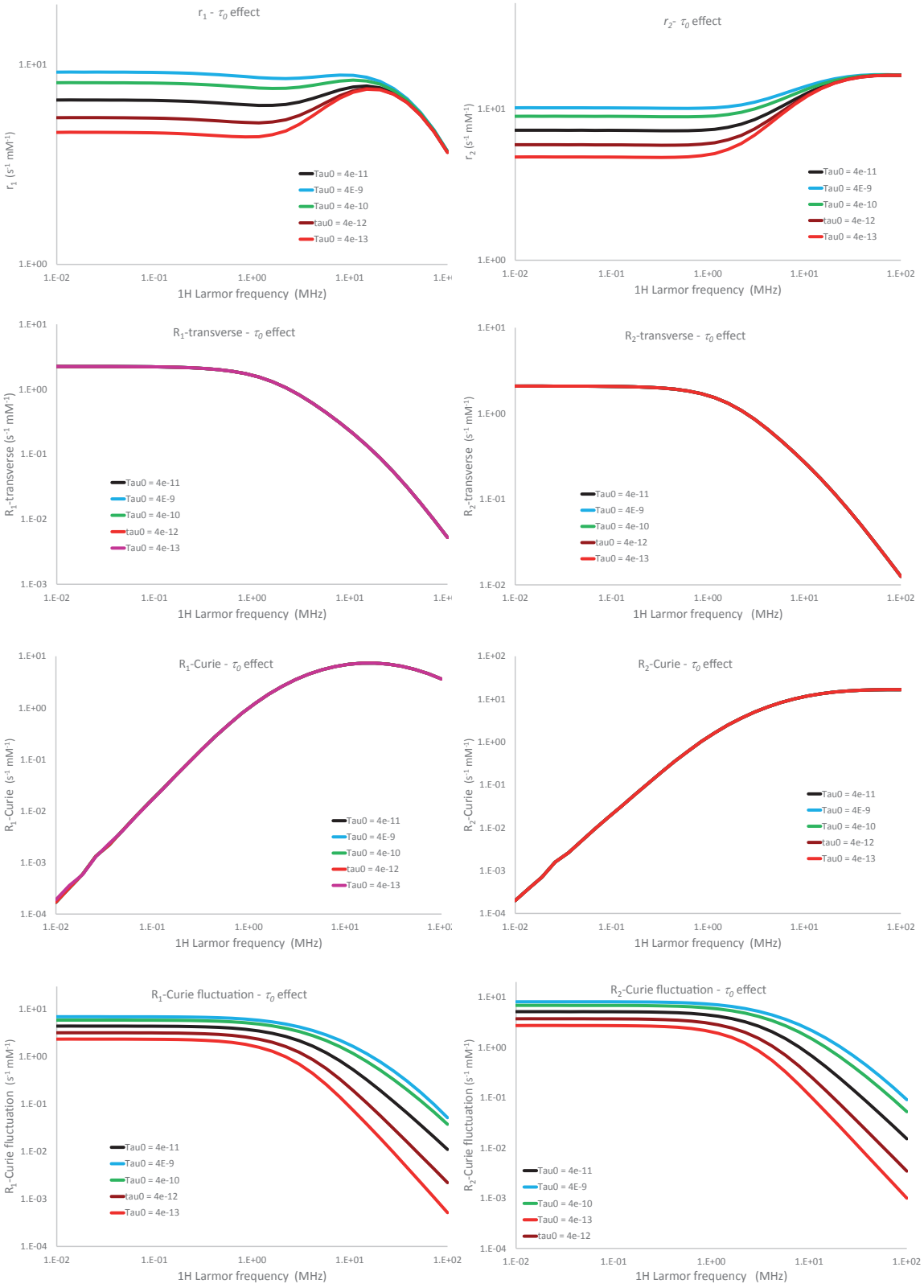

Fig. 5 Effect of τ_0 on the relaxivity r_1 on the left (top) and on the relaxivity r_2 on the right (top), as well as its effect on the three components (transversal term, Curie term and Curie fluctuation term).

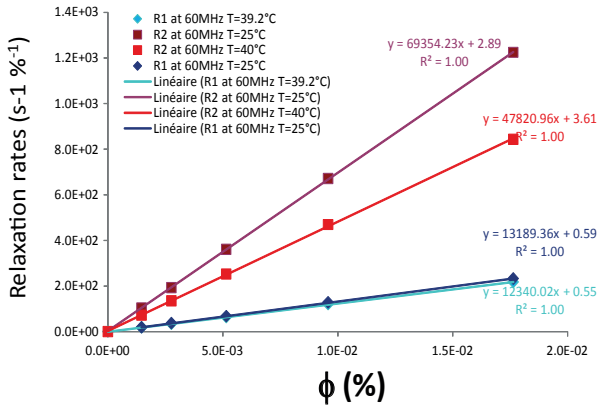

Fig. 6 Variation of the relaxation rates R_1 and R_2 as a function of the volume fraction ϕ in % at 60 MHz for two temperatures ($25\,^{\circ}\mathrm{C}$ and $40\,^{\circ}\mathrm{C}$. The lines represent the linear regression on the experimental data.

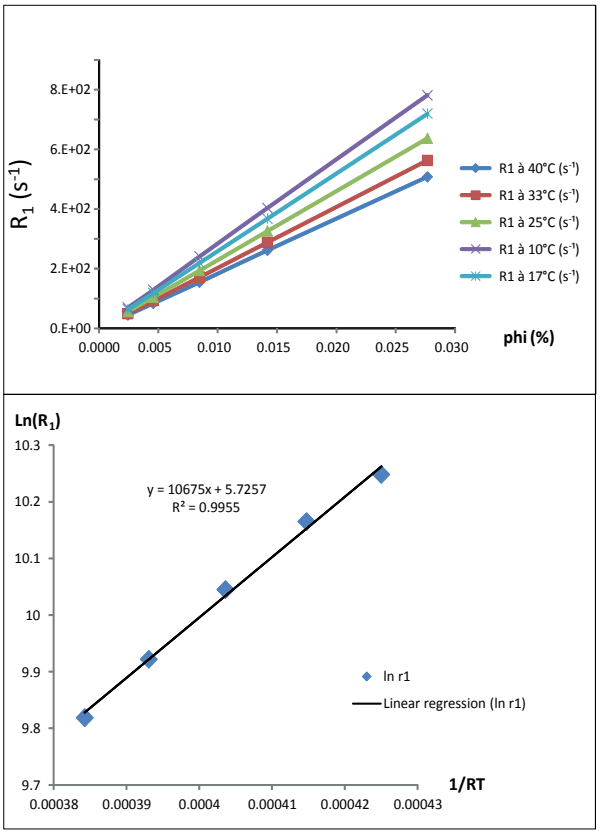

Fig. 7 Top: variations of the relaxation rates R_1 as a function of the volume fraction ϕ in % at 20 MHz for five temperatures (10, 17, 25, 33 and $40\,^{\circ}\mathrm{C}$); the lines represent the linear regression on the experimental data. Bottom: varation of the neperian logarithm of R_1 versus $1/RT$; the line represents the linear regression on the experimental data.

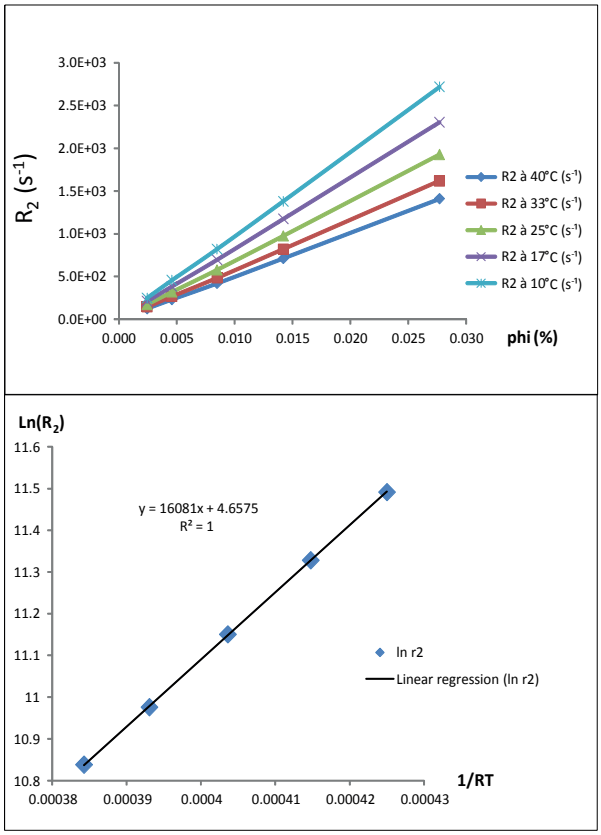

Fig. 8 Top: variations of the relaxation rates R_2 as a function of the volume fraction ϕ in % at 20 MHz for five temperatures (10, 17, 25, 33 and $40\,^{\circ}\mathrm{C}$); the lines represent the linear regression on the experimental data. Bottom: varation of the neperian logarithm of R_2 versus $1/RT$; the line represents the linear regression on the experimental data.